

Grout injection into bed separation to control surface subsidence during longwall mining under villages: case study of Liudian coal mine, China

Dayang Xuan · Jialin Xu

Received: 1 October 2013 / Accepted: 25 February 2014 / Published online: 6 March 2014
© Springer Science+Business Media Dordrecht 2014

Abstract Surface subsidence can cause many environmental problems and hazards (including loss of land area and damage to buildings), and such hazards are particularly serious in coal mining districts. Injecting grout into the bed separation in the overburden has been proposed as an effective control measure against surface subsidence during longwall mining. However, no field trials of this technique have been implemented in mines under villages in China, and thus, its ability to control subsidence in such areas has yet to be demonstrated. In this study, field trials using this technique were carried out during longwall mining under villages in the Liudian coal mine, China. The maximum surface subsidence observed after the extraction was only 0.298 m, which accounts for 10 % of the mining height and is 79 % less than the predicted subsidence. Moreover, no damage occurred to the village buildings either during or after extraction and these buildings remain stable. Thus, this study represents the first successful attempt to control surface subsidence under villages in China using grout injection during longwall mining.

Keywords Coal mining · Surface subsidence control · Grout injection · Bed separation

1 Introduction

Land subsidence is now a global problem (Abidin et al. 2001; Xu et al. 2008; Hsieh et al. 2011) and mostly results from human activity such as groundwater and mineral extraction and the construction of underground facilities. This problem is particularly significant

D. Xuan · J. Xu (✉)
School of Mines, China University of Mining and Technology, Xuzhou 221116, Jiangsu, China
e-mail: xujlcumt@163.com; cumtxjl@cumt.edu.cn

D. Xuan · J. Xu
State Key Laboratory of Coal Resources and Safe Mining, China University of Mining and Technology, Xuzhou 221116, Jiangsu, China



Fig. 1 Environmental problems and/or hazards induced by surface subsidence. **a** Landscape modification in Daliuta coal mine in Shendoing mining district (occurred in 2009), **b** building damage associated with Xuchang coal mine in Zibo mining district (occurred in 2004), **c** waterlogging in farmland surrounding Yangzhuang coal mine in Huaibei mining district (occurred before 2005) and **d** road damage above Taian coal mine in Yangquan mining district (occurred in 2011)

within the coal mining industry. Globally, subsidence due to coal extraction has occurred in every coalfield owing to the caving of the strata overlying the coal seams. In mining districts, voids caused by the extraction of coal propagate gradually to the surface, inducing surface subsidence. Such subsidence occurs in two ways: either as potholes or as troughs, which are expressed as sudden surface settlements over small areas or as large surface depressions, respectively. Pothole subsidence is particularly threatening to human life and the landscape because it occurs typically without prior warning. Surface subsidence can cause many environmental problems and hazards, including landscape modification (Fig. 1a), building damage (Fig. 1b), waterlogging in the subsidence area (Fig. 1c), and road damage (Fig. 1d). For example, severe road damage occurred as a result of sudden pothole subsidence (up to 10 m) induced by underground longwall mining in the Taian coal mine (Fig. 1d) in China, in 2011. Recently in China, problems of surface subsidence have become increasingly serious because of rapid increases in coal production, which reached 3.65 billion t in 2012 (National Bureau of Statistics of China 2013). Such problems are particularly serious in the Huaibei mining district in East China, because this is a densely populated area with more than 300 villages lying above the coal seams. Residents of the area have long experienced serious issues relating to surface subsidence, which threatens lives, infrastructure, and livelihoods; the damage that occurs to buildings because of surface subsidence is particularly common and severe (Julio-Miranda et al. 2012).

For some time, attention has been devoted to the development of measures to control mining-induced surface subsidence, with previous studies covering subsidence prediction (Bahuguna et al. 1991; Nie et al. 2013; Xu et al. 2014), investigation (Can et al. 2013), prevention (Jiřina and Jan 2010), and mitigation (Luo et al. 2003, 2004; Siriwardane et al. 2003). To control surface subsidence induced by mining activities, mining waste and mineral processing by-products can be reused to fill mining voids (Siriwardane et al. 2003; Jiřina and Jan 2010; Bian et al. 2012). For example, grout injection into bed separation (GIBS) during longwall mining has been proposed as a means of preventing subsidence while reusing mining waste (Palarski 1989; Zhao et al. 1995).

Previously, GIBS test cases have been conducted tentatively through trial and error. Moreover, no previous test cases have been able to achieve sufficient control over surface subsidence, and no test cases have investigated the use of GIBS in subsidence control during longwall mining under villages in China. This study tested GIBS under villages during longwall mining, providing guidance and acting as reference for similar trials investigating the mitigation of surface subsidence and building damage in populated coal mining districts.

2 GIBS technique

GIBS involves the injection of fly ash slurry into bed separations by pumping through surface boreholes as the longwall face advances, as shown in Fig. 2. Bed separations are horizontal fractures that occur along the interfaces between weak and strong rock layers during coal extraction (Palchik 2005, 2010; Chen and Guo 2008; Chen and Hu 2009). The compacted fly ash in the bed separation can support the overburden and thus control surface subsidence.

The concept of GIBS was first proposed by researchers in the former Soviet Union, and workers in Poland conducted GIBS field trials with regard to both the underground disposal of waste (e.g., fly ash, tailings) and the control of subsidence (Palarski 1989). The results of

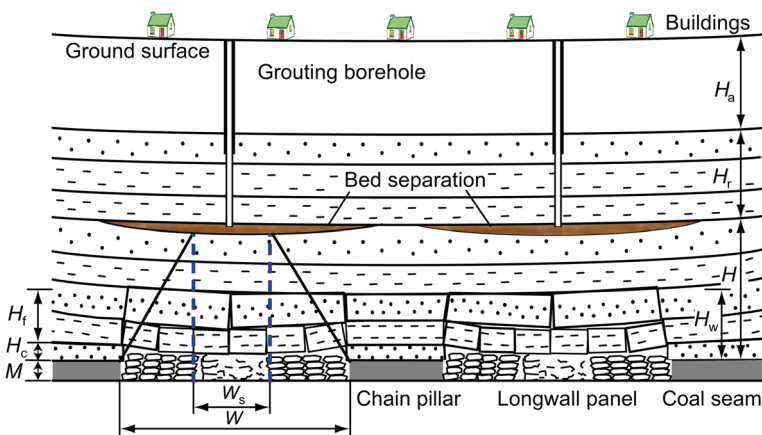


Fig. 2 Schematic cross-section of GIBS. H distance from the grouting position to the coal seam, H_f height of the fractured zone, H_c height of the caved zone, M mining height, H_w height of the fractured water-conducting zone, W_s supporting width of the grouting pillar, W panel width, H_a thickness of the alluvium and H_r total thickness of rock strata above the bed separation

a previous study demonstrated that GIBS could reduce surface deformation by 20–30 % compared with that typically induced by traditional mining with full caving (Palarski 1989), which is an insufficient improvement when mining under villages. In the 1980s, GIBS field trials were implemented in the Laohutai coal mine. This represented the first attempt to control surface subsidence in China (Zhao et al. 1995), which was followed by around ten similar trials in other coal mines, e.g., Xuzhuang and Tangshan (Yang 2002). However, the best result of these GIBS applications indicated that surface subsidence could be reduced by only 41 % (Yang 2002), which was considered still insufficient for meeting the safety requirements for mining under villages. Moreover, in several cases, the application of GIBS failed to mitigate subsidence at all, resulting in skepticism regarding the efficacy of the technique in the Chinese coal mining industry. Research into GIBS has also been performed in Australia (Guo et al. 2005, 2007; Chen and Guo 2008; Chen and Hu 2009). In particular, field tests were conducted at Baal Bone Colliery in 2005, where the overburden depth was just 42 m (Guo et al. 2007). The objective of this field test was not to control surface subsidence but to test the injection system and the injection process after subsidence had fully developed.

For the GIBS trials presented by Yang (2002), none pillar mining method (typically used in China) was adopted, which means no pillar or a narrow pillar (with a width of 5–10 m) was left between adjacent longwall panels. Generally, a good subsidence control effect was achieved during the extraction of the first panel under the injection; however, surface subsidence increased significantly after the extraction of the second panel, although GIBS was also conducted. This can be attributed to the fact that only subcritical mining condition was considered in these trials, which might be true for single panel extraction, while a critical or supercritical mining condition would be met in the general practice for two or more adjacent panels extraction, especially when none pillar mining method was used. As a result, a good subsidence control effect was not achieved in these GIBS trials (Yang 2002). In fact, due to the movement of overburden strata under none pillar mining condition, there was no time for injection during the extraction of the second panel. In addition, the filling ratio (FR), which is defined as the ratio between the injected volume of compacted fly ash and the mined-out volume, only reached 20 % in these trials (Yang 2002).

In this study, the GIBS technique has been further improved to obtain a better subsidence control effect for longwall mining under villages. The principle of the improved GIBS technique can be described as follows: a certain width of grouting pillar can be generated in the center of longwall panel by appropriate selection of the grouting position, and the grouting pillar works the same way as the coal pillar in the partial mining (e.g., room and pillar mining); meanwhile, a chain pillar (generally about 1/4–1/3 of the subcritical panel width, depending on the panel width, the overburden depth and the grouting position) is left between adjacent panels; therefore, in combination with the supporting of the grouting pillars, surface subsidence can be better controlled (refer to Fig. 2). The improved GIBS technique takes advantage of the principle of partial mining and allows a greater FR, ensuring a good subsidence control effect is achievable.

3 Site description

3.1 Location of the study site

The Liudian coal mine is located in Bozhou, Anhui Province, China. It is operated by the Huaibei Mining Group Co., Ltd. and commenced operation in 2009. The villages overlying

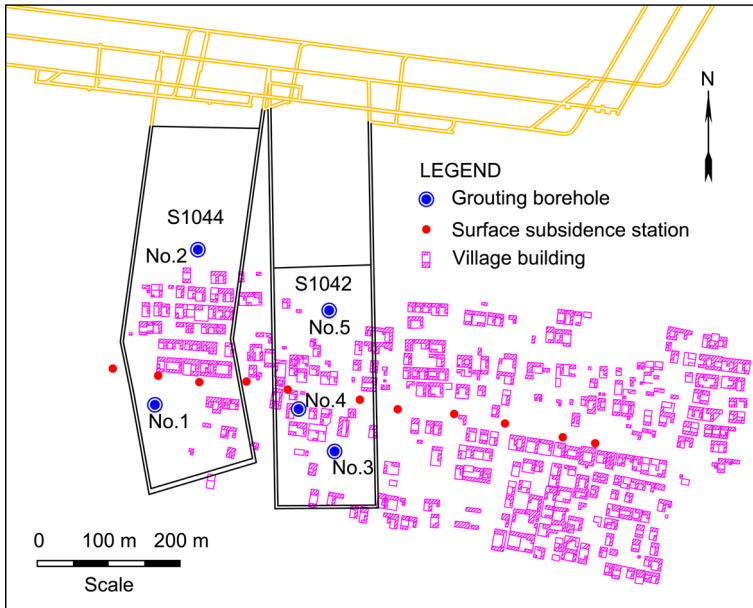


Fig. 3 Plan view of the study site showing surface and underground features

the coal reserves have been affected adversely by the mining activity of the Liudian coal mine, and 58 of the 76 villages within the limits of the mine are located directly above the seam. In particular, the study site selected here (the S104 section, which was mined first) is overlain by two villages (Fig. 3). Together, the two villages comprise 410 households, 1,660 residents, and cover an area of around 33.3 hm². Table 1 presents the percentage of each type of building structure in the two villages.

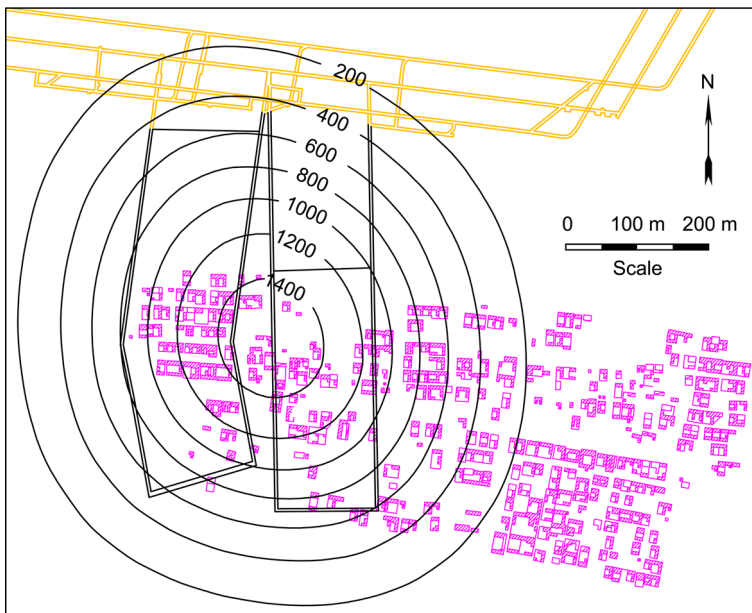
3.2 Surface subsidence prediction

Surface subsidence induced by longwall mining in this region was predicted before the extraction using the probability integral method (PIM) recommended by the State Bureau of Coal Industry (2000). PIM was developed by Chinese researchers Liu and Liao (1965) based on the stochastic medium theory proposed by Litwiniszyn (1958). It is one of the influence function methods, famous for the adoption of the probability integral function as its influence function. PIM is the most popular approach in China. According to PIM, the movement of strata and the surface induced by coal extraction can be considered as the movement of a granular medium, which is a random process following statistical regularity; the entire mining area can be divided into infinite small elements, and surface movement induced by the entire mining area is equal to the sum of that induced by all the elements. Surface subsidence and horizontal displacement induced by an element can be expressed as

$$W_c(x) = \frac{1}{r} \exp\left(-\frac{\pi x^2}{r^2}\right), \tag{1}$$

Table 1 Percentage of each type of building structure present in the two villages studied in the Liudian coal mine region

	One-story brick-concrete structure (%)	Two-story brick-concrete structure (%)	Brick and timber structure (%)	Other (%)
Village A	14	22	59	5
Village B	20	20	58	2

**Fig. 4** Predicted surface subsidence contours for the study site (mm)

$$U_c(x) = -\frac{2\pi Bx}{r^3} \exp\left(-\frac{\pi x^2}{r^2}\right), \quad (2)$$

where $W_c(x)$ and $U_c(x)$ are the surface subsidence and horizontal displacement, respectively, for an arbitrary distance x from the center of the element, r is the radius of major influence, and B is a constant. Here, $r = H_d/\tan\beta$, where H_d is the overburden depth, and $\tan\beta$ is the tangent of the angle of major influence. $B = br$, where b is the horizontal displacement coefficient. According to Eqs. (1) and (2), the surface displacements and deformations of arbitrary points induced by a longwall panel can be calculated.

Subsidence contours were generated for the study site (Fig. 4). It is shown that surface subsidence in the study site would reach a maximum of 1,400 mm, sufficient to cause serious damage to the land surface and to buildings; thus, many buildings in the area would be in danger of collapse. Moreover, it is likely that the farmland in the subsidence trough would become filled with groundwater, making it uncultivable. This predicted level of surface subsidence is not permitted in villages; in general, coal extraction in the area would require the removal of these two villages, which would have a considerable adverse effect on the residents. Furthermore, preliminary estimates suggest that such removal would cost up to 70 million RMB, which would make the Liudian coal mine uneconomic. These

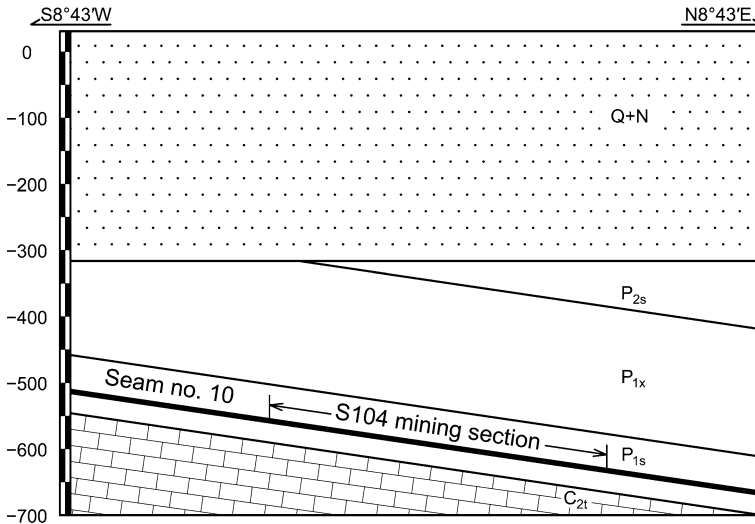


Fig. 5 Geological section of the study area. C_{2t} Taiyuan Formation (Upper Carboniferous), P_{1s} Shanxi Formation (Lower Permian), P_{1x} Xiashihezi Formation (Lower Permian), P_{2s} Shangshihezi Formation (Upper Permian) and Q + N Cenozoic Tertiary–Quaternary

circumstances prompted the implementation of GIBS tests, both to control surface subsidence and to mitigate building damage caused by longwall mining.

3.3 Geology and mining conditions

The Liudian coal mine is located in the Huaibei plain. The landscape in this area is flat with an average elevation of 30 m above sea level. The S104 mining section is located at the south of the mine. The surface area comprises farmland and villages. The strata sequence from bottom to top is: Taiyuan Formation (Upper Carboniferous) (C_{2t}), Shanxi Formation (Lower Permian) (P_{1s}), Xiashihezi Formation (Lower Permian) (P_{1x}), Shangshihezi Formation (Upper Permian) (P_{2s}) and Cenozoic Tertiary–Quaternary (Q + N) (Fig. 5). The mine is totally covered by Cenozoic strata. The coal-bearing strata are the Shanxi Formation (Lower Permian), which exhibits a uniclinal structure with an average angle of 15°. The main dip direction is toward the NNW. Faults are well developed in the mine. The coal seam extracted in section S104 is seam no. 10, and the exploitable thickness of which varies between 0.70 and 3.43 m. On average, within the study area, this seam is overlain by 620 m of overburden, including approximately 350 m of alluvium resting unconformably on the Upper Paleozoic strata.

The S104 section includes two panels: S1044 (155 m wide and 407 m long) and S1042 (145 m wide and 337 m long). The chain pillar has an irregular shape, with a width of 32–54 m (mean width: 43 m), and the roof comprises fine- to medium-grained sandstone and mudstone (Fig. 6).

4 GIBS scheme

4.1 Grouting borehole layout

The grouting borehole layout includes the grouting position and borehole spacing. To achieve a large grouting volume, the grouting position should be located in the overlying

Thickness (m)	Cover depth (m)	Lithology	Columnar
350.00	350.00	Alluvium	
6.39	356.39	Sandstone	
6.56	362.95	Mudstone	
1.05	364.00	Sandstone	
3.42	367.42	Mudstone	
1.24	368.66	Sandstone	
5.33	373.99	Mudstone	
23.72	397.71	Sandstone	
4.18	401.89	Mudstone	
1.57	403.46	Sandstone	
2.28	405.74	Mudstone	
5.32	411.06	Sandstone	
3.42	414.48	Mudstone	
7.13	421.61	Sandstone	
4.66	426.27	Mudstone	
27.81	454.08	Sandstone	
9.94	464.02	Mudstone	
1.71	465.73	Sandstone	
2.38	468.11	Mudstone	
11.90	480.01	Sandstone	
4.42	484.43	Mudstone	
12.10	496.53	Sandstone	
7.47	504.00	Mudstone	
14.21	518.21	Sandstone	
4.84	523.05	Mudstone	
2.06	525.11	Magmatic rock	
2.20	527.31	Carbonite	
0.34	527.65	Mudstone	
0.38	528.03	Seam no. 7	
3.80	531.83	Mudstone	
25.90	557.73	Sandstone	
2.29	560.02	Mudstone	
21.86	581.88	Sandstone	
3.49	585.37	Mudstone	
33.40	618.77	Sandstone	
7.63	626.40	Mudstone	
3.00	629.40	Seam no. 10	

Fig. 6 Borehole log for the study site (not to scale)

region of maximum subsidence, which is typically defined (at least in China) using the angle of full subsidence (State Bureau of Coal Industry 2000). Then, the grouting position (i.e., the bottom of the grouting borehole) can be described as follows:

$$H \leq \frac{W}{2} \tan \varphi, \tag{3}$$

where H is the distance from the grouting position to the coal seam W is the width of longwall panel; φ is the angle of full subsidence, which is defined as the angle between a line joining the edge of the flat part of the subsidence trough to the edge of the extraction zone and the coal seam layer (State Bureau of Coal Industry 2000). This angle is used primarily in China, and it corresponds approximately to the complementary angle of the angle of draw used elsewhere, e.g., the UK and the USA (Harrison 2011). Based on field observations, the empirical values for the angle of full subsidence in different mining districts have been proposed by the State Bureau of Coal Industry (2000).

Furthermore, the grouting position must not intersect with the fractured water-conducting zone; such an intersection could result in an inrush of injected slurry at the underground working face. Therefore, the grouting position should be located some distance above the fractured water-conducting zone, as follows:

$$H \geq H_w + H_p, \tag{4}$$

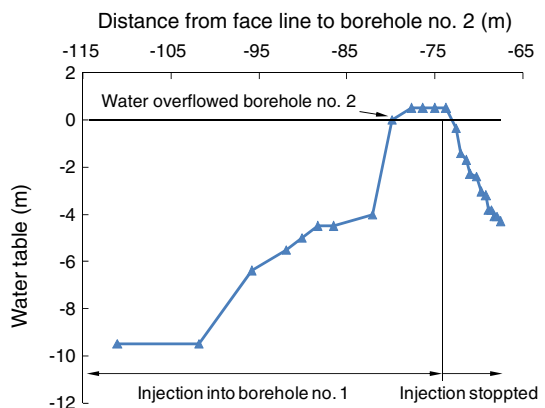
where H_w is the height of the fractured water-conducting zone, which can be evaluated based on data from the State Bureau of Coal Industry (2000) or determined by field observation. H_p is a safe rock strata thickness and can be chosen as 1–1.5 times H_w . Then, the borehole depth can be expressed as the difference between the overburden depth and the distance from the grouting position to the seam.

The grouting position was calculated based on Eqs. (3) and (4) using the parameters listed in Table 2. As mentioned previously, the angle of full subsidence for the Liudian

Table 2 The calculated distance from the grouting position to the coal seam for the grouting boreholes above panels S1044 and S1042

	φ (°)	W (m)	H_{max} (m)	M (m)	H_w (m)	H_p (m)	H_{min} (m)
Panel S1044	60.0	154.0	134.0	3.0	41.3	51.6	92.9
Panel S1042	60.0	145.0	125.6	3.2	42.3	52.9	95.2

Fig. 7 Water table in borehole no. 2 during the injection of grout into borehole no. 1



coal mine was obtained from empirical data collected in the Huaibei mining district, and H_w was set based on information from the State Bureau of Coal Industry (2000). H_p was set to 1.25 times H_w .

The borehole spacing should be determined mainly based on the grouting diffusion radius as well as the positions of surface structures. In this study, the grouting diffusion radius was determined from field observations of panel S1044. Two boreholes (nos. 1 and 2) with a spacing of 225 m were drilled from the surface above this panel (Fig. 3); this spacing was primarily determined based on the positions of village buildings. During injection into borehole no. 1, the water table in borehole no. 2 was monitored to investigate the grouting diffusion radius (Fig. 7). During the observation period, the water table in borehole no. 2 rose dramatically when the face line was 101.8 m in by borehole no. 2 and the water (containing a small amount of fly ash) overflowed borehole no. 2 when the line was 79.9 m in by borehole no. 2. The water table began to decline as soon as grout injection into borehole no. 1 ceased. The results obtained indicate a grouting diffusion radius of up to 225 m.

The locations of the boreholes above panel S1042 were determined based on the positions of surface structures and the grouting diffusion radius observed from panel S1044. Three boreholes (nos. 3–5) with a maximum spacing of 130 m were drilled above panel S1042 (Fig. 3). The grouting diffusion radius was verified by observing the water overflow rate in borehole no. 5 (Fig. 8). Before the injection of grout into boreholes 3 and 4, the water table in borehole no. 5 was below the surface level, whereas during the injection of grout into boreholes 3 and 4, the water (containing a small amount of fly ash)

Fig. 8 Water overflow rate in borehole no. 5 during the injection of grout into boreholes 3 and 4

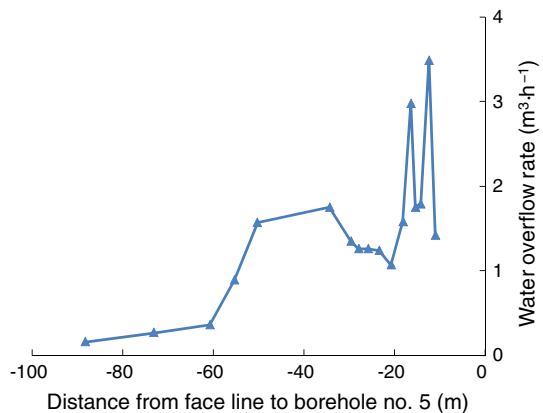


Table 3 Locations and depths of the grouting boreholes designed for the study site

	No. 1	No. 2	No. 3	No. 4	No. 5
Distance to the opening (m)	113.8	338.8	81.6	141.0	271.0
Distance to the head gate (m)	124.8	65.8	84.2	34.5	70.6
Distance to the tail gate (m)	31.0	90.8	60.0	109.3	72.3
Borehole depth (m)	464.8	505.1	465.0	446.7	502.0
H (m)	143.0	130.9	92.1	123.9	103.2

in borehole no. 5 began to overflow at a rate of 0.16 m³/h when the face line was 88.2 m inby borehole no. 5. The water overflow rate reached a maximum of 3.49 m³/h when the face line was 12.4 m inby borehole no. 5, demonstrating that the grouting diffusion radius was considerably >130 m.

Detailed information for all five boreholes is provided in Table 3. It should be noted that the actual value of *H* for borehole no. 1 is slightly greater than the calculated *H*_{max} listed in Table 2. This is because drilling for this borehole was halted because of the total loss of drilling fluid.

4.2 Grouting system

Fly ash produced by the Linhuan Joinlion Power Co., Ltd. was selected as the grouting material. The haul distance was 57 km, and the particle size distribution of the fly ash used is shown in Table 4. The fly ash and water were mixed to form a slurry.

Figure 9 illustrates the designed grouting system. This system has the capability of 1,400 m³/day (which is equal to approximately 700 m³ of compacted fly ash daily).

To support the overlying strata and to control surface subsidence, the slurry pressure in the bed separation should be equal to or larger than the gravitational force exerted by the overburden above the bed separation. The slurry pressure in the bed separation and the grouting pressure at the top of the borehole can be calculated as follows:

$$P = \gamma_a H_a + \gamma_r H_r, \tag{5}$$

$$P_1 = P - \gamma(H_a + H_r), \tag{6}$$

where *P* is the slurry pressure in the bed separation (MPa); *P*₁ is the grouting pressure at the top of the borehole (MPa); γ_a , γ_r and γ are the unit weights of the alluvium (MN/m³), rock strata (MN/m³) and slurry (MN/m³), respectively; *H*_a is the thickness of the alluvium above the bed separation; and *H*_r is the total thickness of the rock strata above the the bed separation. The grouting pressure was calculated to be no <4.9 MPa based on Eqs. (5) and (6).

Table 4 Particle size distribution of the fly ash for the slurry preparation

Particle size (μm)	<25	25–45	45–75	75–100	>100
Mass percentages (%)	75.84	14.04	8.20	1.38	0.54

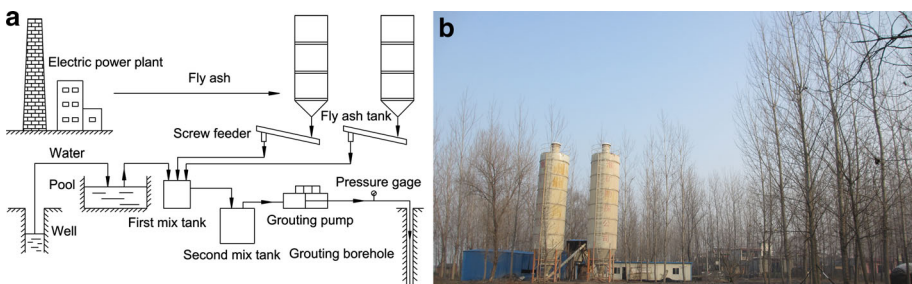


Fig. 9 Grouting system. **a** Schematic diagram and **b** photograph

Table 5 Grouting volume in each grouting borehole above the S104 mining section

	No. 1	No. 2	No. 3	No. 4	No. 5
Volume of compacted fly ash injected (m ³)	43,624	23,724	37,690	27,608	37,005

4.3 Grouting process

The grouting process is summarized as follows. When the face line is about 40 m inby each borehole, the injection of water or low-concentration fly ash slurry could be initiated through the borehole. Conversely, when the face line is outby each borehole, a designated concentration of slurry should be injected as the grouting pressure drops.

During grouting and extraction, the mining speed should be coordinated with the grouting rate. Thus, to achieve the desired effect of subsidence control, the mining speed was limited to a maximum of 3 m/day in reference to the grouting rate, and the actual panel advance must slow down when the actual grouting rate drops unexpectedly.

5 Surface subsidence control effect

Grout injection was first conducted for panel S1044. The grout injection for this panel proceeded from September 8, 2009, to June 6, 2010, with a total grouting volume of 67,348 m³ (compacted fly ash). The grouting of panel S1042 commenced on December 1, 2011, reaching a total grouting volume of 102,303 m³ (compacted fly ash) by August 5, 2012. The total grouting volume in section S104 accounted for 43.1 % of the volume of the gob. The grouting volumes achieved through each borehole are listed in Table 5.

5.1 Surface displacements

The observations of surface subsidence (stations shown in Fig. 3) were conducted during and after the extraction. The horizontal displacement was measured using the total station after the extraction. During and after the extraction, precise leveling was conducted using optical leveling apparatus and a level rod.

The final horizontal and vertical displacements (i.e., the subsidence) are listed in Tables 6 and 7, respectively. In Table 6, the positive values represent a horizontal displacement toward the east or north, and negative values represent movement in the opposite sense. In Table 7, positive values represent a downward vertical displacement of vector points, i.e., the surface station subsides. Figures 10 and 11 depict the horizontal and vertical displacement vectors. The maximum horizontal displacement and subsidence are 0.109 and 0.298 m, respectively.

5.2 Surface deformations

In addition to the vertical and horizontal displacements, there are three primary indicators describing surface deformations: inclination (i), curvature (K) and horizontal strain (ϵ). All of these deformations can be derived from vertical or horizontal displacement.

According to the subsidence of the stations (Table 7), the inclinations and curvatures can be obtained (Tables 8, 9). The positive inclination indicates that the rod-shaped objects (e.g., poles) dump toward the positive direction of the x axis. It can be seen from Tables 8

Table 6 Final horizontal displacement vectors of surface stations in the S104 mining section

Point no.	V1	V2	V3	V4	V5	V6	V7	V8	V9	V10	V11
Y (east) (m)	0.038	0.055	0.069	0.063	0.039	-0.079	-0.099	-0.083	-0.050	-0.028	-0.022
X (north) (m)	0.005	0.006	0.008	0.010	0.002	0.044	0.044	0.030	0.019	0.011	0.009
Vectors (m)	0.038	0.056	0.070	0.064	0.039	0.091	0.109	0.088	0.053	0.030	0.024

Table 7 Vertical displacements of surface stations in the S104 mining section (m)

Point no.	V1	V2	V3	V4	V5	V6	V7	V8	V9	V10	V11
I	0.117	0.107	0.127	0.116	0.111	0.093	0.063	0.043	0.035	0.023	0.012
II	0.180	0.197	0.235	0.263	0.298	0.287	0.235	0.179	0.130	0.089	0.071

“I” and “II” represent surface subsidence after the extraction of panels S1044 and S1042, respectively

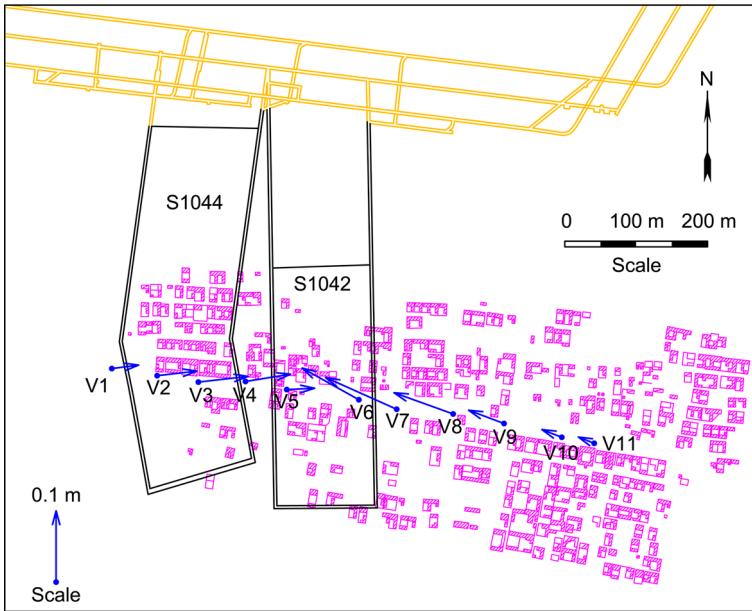


Fig. 10 Horizontal displacement vectors of surface stations in the S104 mining section

and 9 that the maximum inclination and curvature are 0.96 mm/m (between V6 and V7) and 0.011 mm/m² (between V5 and V7), respectively.

Similarly, using the horizontal displacements (Table 6), the strains can be obtained (Table 10). The positive horizontal strain suggests the occurrence of tensile deformation, whereas negative values represent the compressive deformation. The maximum tensile and compressive strains are 0.41 mm/m (i.e., V8–V9) and –1.16 mm/m (i.e., V5–V6), respectively.

5.3 Limit angle

The limit angle (δ_0) is used to define the border of the subsidence trough (Fig. 12), which can be calculated as

$$\delta_0 = \arctan \frac{H_d - H_a}{X_0 - H_a \cot \psi_a}, \tag{7}$$

where X_0 is the horizontal distance from the subsidence trough border to the panel boundary, and ψ_a is the movement angle of the alluvium. According to the State Bureau of Coal Industry (2000), the value of ψ_a was taken as 45° in this study.



Fig. 11 Vertical displacement vectors of surface stations in the S104 mining section

Table 8 Final inclinations in the S104 mining section

No.	V1– V2	V2– V3	V3– V4	V4– V5	V5– V6	V6– V7	V7– V8	V8– V9	V9– V10	V10– V11
Inclinations (mm/m)	0.28	0.66	0.42	0.59	−0.11	−0.96	−0.78	−0.62	−0.49	−0.38

Table 9 Final curvatures in the S104 mining section

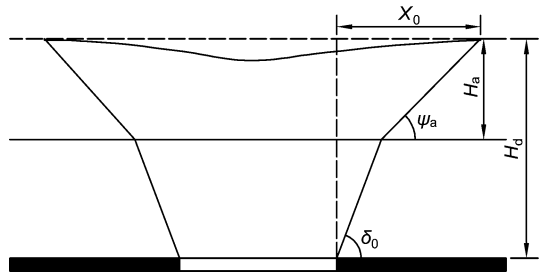
No.	V1– V2–V3	V2– V3–V4	V3– V4–V5	V4– V5–V6	V5– V6–V7	V6– V7–V8	V7–V8– V9	V8–V9–V10	V9–V10– V11
Curvatures (mm/m ²)	0.006	−0.004	0.003	−0.009	−0.011	0.003	0.002	0.002	0.002

Table 10 Final strains in the S104 mining section

No.	V1– V2	V2– V3	V3– V4	V4– V5	V5– V6	V6– V7	V7– V8	V8– V9	V9– V10	V10– V11
Strains (mm/m)	0.29	0.24	−0.09	−0.41	−1.16	−0.37	0.23	0.41	0.27	0.13

Considering measurement error, the point with a subsidence value of 0.01 m is generally treated as the border of the subsidence trough (State Bureau of Coal Industry 2000). After the extraction of panel S1044, the subsidence of station V11 was 0.012 m (Table 7), indicating

Fig. 12 Schematic of the limit angle in strike direction. δ_0 limit angle, X_0 horizontal distance from the border of subsidence trough to the boundary of the panel, ψ_a movement angle of the alluvium, H_a thickness of the alluvium and H_d overburden depth



the position of station V11 could be approximately treated as the subsidence trough border and used for the calculation of δ_0 . By substituting $H_d = 589$ m, $H_a = 350$ m, $X_0 = 480$ m and $\psi_a = 45^\circ$ into Eq. (7), the limit angle (δ_0) is suggested to be 61.5° .

6 Effect of injection on subsidence control

6.1 GIBS subsidence

Surface subsidence is the result of the development of mining-induced voids, one of which is the horizontal fracture along the rock layer interface at the bed separation. During coal extraction, bed separation generally occurs along the interface between soft and hard rock layers (Palchik 2005, 2010; Chen and Guo 2008) and develops from lower position toward upper position as the longwall panel advances (Palchik 2003; Jia et al. 2008). And the grouting can be conducted when the bed separation develops into the borehole range. During the injection, the bed separation at the injection level will be further developed in terms of both horizontal and vertical range owing to the injection pressure, which in turn increases the grouting volume. Meanwhile, the gob under the injection level will be compacted gradually as a result of the high injection pressure and the large injection volume. Consequently, the pre-developed separations below the injection level will be closed gradually due to this kind of compaction. In other words, there will be no bed separations above the caved zone. Similarly, the grouting will also exert a lifting force to its overburden strata, and the subsidence of its overburden strata and the surface can be assumed equal.

Therefore, the mining height can be divided into three components, which can be written as

$$M = S_{cmin} + S_{bmax} + S_{smax}, \quad (8)$$

where S_{cmin} is the minimum residual thickness of the voids in the caved zone, S_{bmax} is the maximum thickness of the injection body in the bed separation, which also represents the aperture of the horizontal fracture at the bed separation under the injection, and S_{smax} is the maximum surface subsidence. Here, S_{cmin} can be expressed as

$$S_{cmin} = H_c (K_p' - 1), \quad (9)$$

where H_c is the height of the caved zone (Fig. 2), and K_p' is the residual bulking factor of the caved rock in the gob. It should be noted that the actual mechanism of mining-induced surface subsidence is very complex, and Eq. (8) is just simplified for this analysis.

Substituting Eq. (9) into Eq. (8), S_{smax} can be determined

$$S_{smax} = M - H_c \left(K'_p - 1 \right) - S_{bmax}. \tag{10}$$

It can be seen from Eq. (10) that S_{bmax} is a significant parameter in terms of mitigating surface subsidence. Thus, it is vital to determine the distribution of the injection body thickness in the bed separation (i.e., the aperture of the injected bed separation) so as to evaluate surface subsidence control effect.

6.2 Aperture of bed separation

As mentioned above, the thickness of the injection body in the bed separation represents the final aperture of the bed separation with injection. However, it varies significantly with the aperture of the mining-induced horizontal fracture without injection.

6.2.1 Aperture of mining-induced horizontal fracture without injection

Field measurements and numerical simulations (Teng and Yan 1999; Xu et al. 2003; Palchik 2003, 2010; Chen and Guo 2008; Jia et al. 2008) have demonstrated that, without injection, the mining-induced horizontal fracture at the bed separation experiences a dynamic development process (i.e., initiation, expansion and closure) as the longwall face advances and that the maximum aperture of the mining-induced horizontal fracture is relatively small. For example, Teng and Yan (1999), Jia et al. (2008) and Palchik (2010) measured the aperture of the mining-induced horizontal fracture in the Tangshan coal mine in China, the Zhongjiashan coal mine in China and the Donetsk Coal Basin in Ukraine, respectively, and found that the averages of the mining-induced horizontal fracture aperture were 0.040, 0.147 and 0.115 m, respectively, and then the ratios of the mining-induced horizontal fracture aperture to the mining height could be determined for the three cases which were 0.02, 0.015, and 0.09, respectively (Fig. 13).

6.2.2 Aperture of bed separation with injection

When the injection is conducted, the bed separation will be well developed due to high injection pressure and increased grouting volume accordingly. Consequently, the bed separation will be filled with the injection material, which prevents it from closure. Actually, the thickness of the injection body is the difference between the subsidence of the first strata underlying and overlying the bed separation, which can be calculated based on the influence function (State Bureau of Coal Industry 2000). Therefore, the aperture of the bed separation (i.e., the thickness of the injection body) can be expressed as

$$S_b(x) = \frac{S_{bmax}}{2} \left\{ \operatorname{erf} \left(\frac{\sqrt{\pi}}{r} x \right) + \operatorname{erf} \left[\frac{\sqrt{\pi}}{r} (W - x) \right] \right\}, \tag{11}$$

where $S_b(x)$ is the thickness of the injection body at location x in the bed separation (the origin is above the left edge of the panel), and it also represents the aperture of the bed separation at location x under the injection. Here, $\operatorname{erf}(x)$ is the error function defined as

$$\operatorname{erf}(x) = \frac{2}{\sqrt{\pi}} \int_0^x e^{-\lambda^2} d\lambda. \tag{12}$$

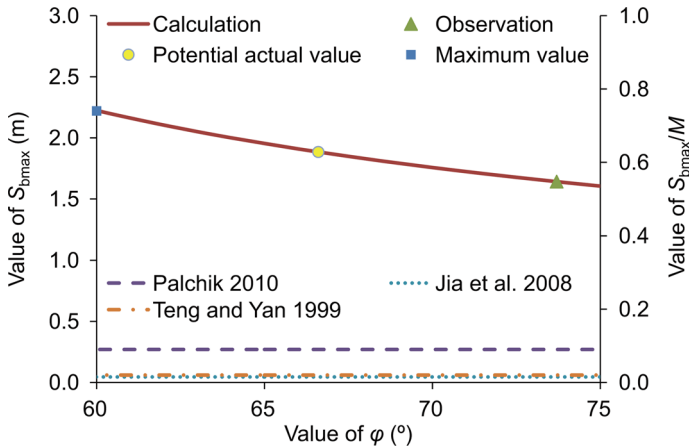


Fig. 13 Calculated and observed bed separation aperture with injection in this study, and the mining-induced horizontal fracture aperture without injection, observed by Teng and Yan (1999), Jia et al. (2008) and Palchik (2010). Potential actual value refers to the inferred maximum thickness of the injection body in the bed separation with injection in this study. Without injection, values of S_{bmax} and S_{bmax}/M have nothing to do with the value of ϕ . S_{bmax} mining-induced horizontal fracture aperture without injection or the bed separation aperture with injection, M mining height and ϕ angle of full subsidence

Because the error function $\text{erf}(x)$ does not have a primitive function, an analytical solution is unavailable to Eq. (11). Furthermore, it is difficult to determine the radius of major influence (r) of the rock strata above and below the bed separation. Therefore, a simplified and approximate calculation method has been proposed in this study. The distribution pattern of the injection body in the bed separation can be treated as an inverted trapezoid, whose upper base, lower base and depth are given by the supporting width of the grouting pillar (W_s), the panel width (W) and S_{bmax} , respectively. Here, the supporting width of the grouting pillar can be given as

$$W_s = W - \frac{2H}{\tan \phi}. \tag{13}$$

Therefore, $S_b(x)$ can be expressed as

$$S_b(x) = \begin{cases} \frac{S_{bmax}x}{H/\tan \phi}, & x < H/\tan \phi, \\ S_{bmax}, & H/\tan \phi \leq x \leq W - H/\tan \phi, \\ -\frac{S_{bmax}x}{H/\tan \phi} + \frac{S_{bmax}W}{H/\tan \phi}, & x > W - H/\tan \phi. \end{cases} \tag{14}$$

The grouting volume (Q) can also be obtained as

$$Q = L \frac{(W_s + W)S_{bmax}}{2}, \tag{15}$$

where L is the panel length. To evaluate the degree of filling, FR (α) was used in this study and is defined as

$$\alpha = \frac{Q}{LMW}. \tag{16}$$

Substituting Eqs. (13) and (16) into Eq. (15), then S_{bmax} and S_{bmax}/M can be expressed as

$$S_{bmax} = \frac{MW\alpha}{W - H/\tan \varphi}, \tag{17}$$

$$\frac{S_{bmax}}{M} = \frac{W\alpha}{W - H/\tan \varphi}. \tag{18}$$

It can be seen that S_{bmax} and S_{bmax}/M can be calculated from M , W , α , H and φ , of which the first four are the actual longwall and grouting parameters, whereas an empirical value can be used for the last parameter. Regarding the value of H , although the values are presented in Table 3, results of an investigation borehole revealed that the actual value of H was 105 m; the investigation borehole close to borehole no. 3 was completed in September 2013. As for φ , the empirical value of 60° was used for the calculation (State Bureau of Coal Industry 2000).

Substituting $\alpha = 43.1\%$, $M = 3.0$ m, $W = 145$ m, $H = 105$ m and $\varphi = 60^\circ$ into Eqs. (17) and (18), it can be obtained that $S_{bmax} = 2.22$ m and $S_{bmax}/M = 0.74$. However, results from the investigation borehole indicated that $S_{bmax} = 1.64$ m and $S_{bmax}/M = 0.55$ (Fig. 13). The discrepancy between the calculated and observed values of S_{bmax} can be attributed to the increased value of φ for the strata below the bed separation due to the compaction generated by injection. Therefore, the calculated value of S_{bmax} is larger than the actual value. Meanwhile, it is believed the investigated value of $S_{bmax} = 1.64$ smaller than the actual value due to the core recovery rate (87.2 %). By recognizing that the ratio of the investigated S_{bmax} to the calculated S_{bmax} $1.64/2.22 = 74\%$ is close to the core recovery rate, it is thought that the actual value of S_{bmax} is between 1.64 and 2.22 m (Fig. 13). Taking the core recovery rate of 87.2 %, it is reasonable to calculate the potential actual value of S_{bmax} as $S_{bmax} = 1.64/87.2\% = 1.88$ m, with $S_{bmax}/M = 0.63$ and $\varphi = 66.6^\circ$.

According to the measurements of Teng and Yan (1999), Jia et al. (2008) and Palchik (2010), 0.042 can be taken as a reasonable estimate of the ratio of the mining-induced horizontal aperture to the mining height without injection. With injection, the ratio was 0.63, which is 15 times of the value without injection, indicating that bed separation was clearly expanded.

Substituting $S_{bmax} = 1.88$ m and $\varphi = 66.6^\circ$ into Eq. (14), the thickness of the injection body in the bed separation above panel S1042 can be expressed as

$$S_{b(x)} = \begin{cases} 0.0414x, & x < 45.4, \\ 1.88, & 45.4 \leq x \leq 99.6, \\ -0.0414x + 6, & x > 99.6. \end{cases} \tag{19}$$

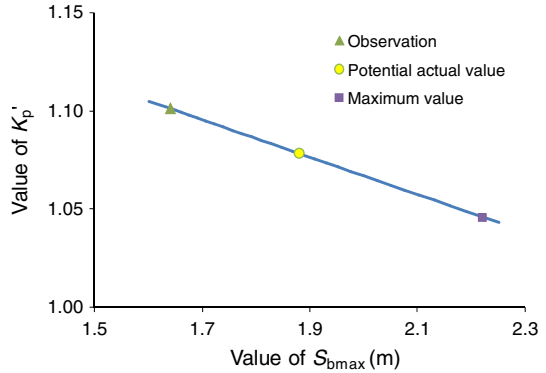
And the total volume of the bed separation above panels S1044 and S1042 is $169,651 \text{ m}^3$.

6.3 Effect of S_{bmax} on subsidence control

6.3.1 Residual voids in overburden

It is known from Eq. (10) that the residual bulking factor (K_p') also affects final surface subsidence and can be expressed as

Fig. 14 Relationship between the calculated residual bulking factor of the caved rock in the gob (K'_p) and the maximum thickness of the injection body in the bed separation (S_{bmax}). Potential actual value refers to the inferred maximum thickness of the injection body in the bed separation with injection in this study



$$K'_p = \frac{M - S_{bmax} - S_{smax}}{H_c} + 1. \tag{20}$$

Substituting $M = 3.0$ m, $S_{smax} = 0.298$ m, $H_c = 10.51$ m (investigation borehole result) and $S_{bmax} = 1.64\text{--}2.22$ m into Eq. (20), it can be obtained that $K'_p = 1.046\text{--}1.101$ (Fig. 14). According to Peng and Chiang (1984), for the mudstone immediate roof that is the case of the S104 mining section, 1.05–1.10 is accepted as a reasonable estimate of the value of K'_p . Meanwhile, Deng et al. (1998) measured the value of K'_p in the Yangquan no. 1 coal mine, China, and concluded that the average value of K'_p varied between 1.03 and 1.05. Therefore, the calculated value of K'_p in this study agrees with the empirical values 1.03–1.10 (Peng and Chiang 1984; Deng et al. 1998), demonstrating that the center of the gob was compacted by the injection and the bed separation was fully filled. On the other hand, it can be seen from Fig. 15 that the maximum grouting pressures for all boreholes had exceeded the pre-set values, indicating the bed separations were well filled for all boreholes.

6.3.2 Comparison of surface subsidence both with and without injection

Without injection, the mining height can be divided into four components: the predicted maximum surface subsidence (S_{sp}), the residual voids of the caved rock, the residual voids of the fractured zone and the apertures of the mining-induced horizontal fractures above the fractured zone (S_{hp}), which can be written as

$$M = S_{sp} + H_c(K'_{pp} - 1) + H_f(K'_{fp} - 1) + S_{hp}, \tag{21}$$

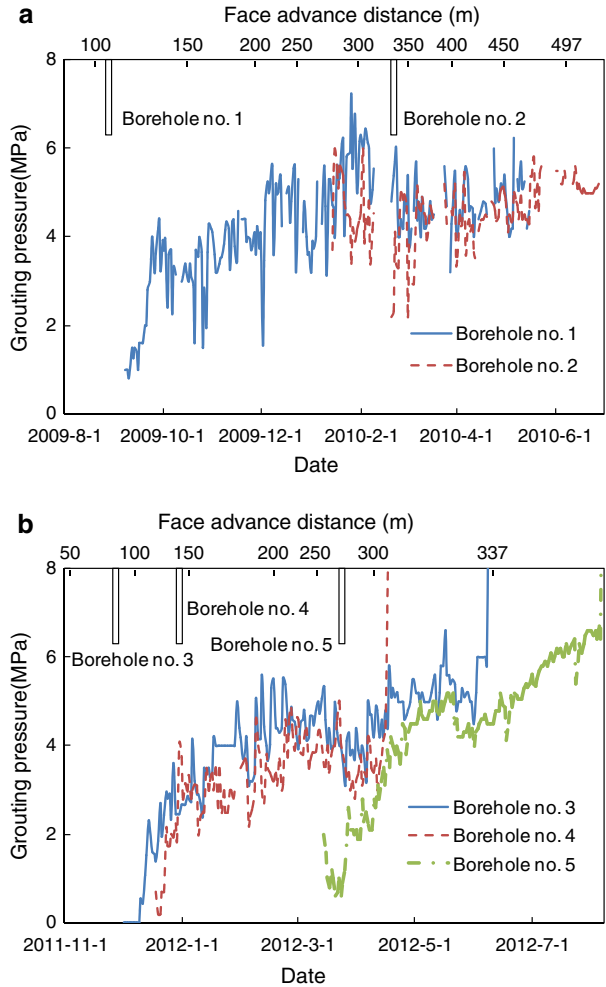
where K'_{pp} and K'_{fp} are the bulking factors of the caved zone and the fractured zone without injection, respectively. Without considering the residual voids of the fractured zone, the predicted maximum surface subsidence can be expressed as

$$S_{sp} = M - H_c(K'_{pp} - 1) - S_{hp}. \tag{22}$$

Meanwhile, the horizontal fractures were not injected and the voids in the bed separation would finally be transferred to the surface, resulting into a value of S_{hp} being approximately zero. Therefore, S_{sp} changes into the following form

$$S_{sp} = M - H_c(K'_{pp} - 1). \tag{23}$$

Fig. 15 Grouting pressure. **a** During injection into panel S1044 and **b** during injection into panel S1042



Substituting $S_{sp} = 1.4$ m, $H_c = 10.51$ m, $M = 3.0$ m into Eq. (23), it can be obtained that $K'_{pp} = 1.152$. By comparing Eq. (10) with Eq. (23), after the injection, it can be seen that S_{bmax} is composed of two parts: one is the compression to the caved rock, reducing the value of K'_p from 1.152 to 1.078, and the other is the reduction in surface subsidence (1.102 m), i.e., the subsidence is reduced from the predicted 1.4 m to the measured 0.298 m (Fig. 16), which is 79 % less than predicted. Ground observations also indicated that there was no damage to the buildings in the villages during and after the mining activity, ensuring the safety of local residents and demonstrating a good subsidence control effect has been achieved.

6.4 Effect of FR on subsidence control

FR is an important indicator reflecting S_{bmax} , which is convenient to use in the engineering practice. It is very important in GIBS projects to evaluate the project quality. Generally, the higher the value of FR, the better the subsidence control effect. Regarding longwall mining

Fig. 16 Comparison of predicted and observed final surface subsidence before and after injection

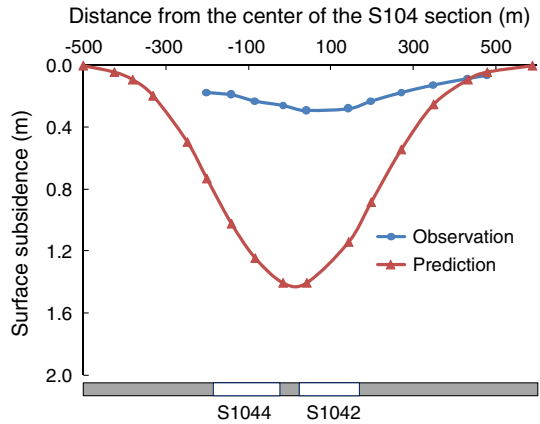
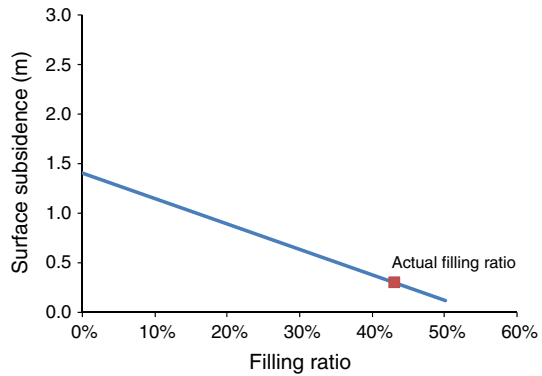


Fig. 17 Relationship between final maximum surface subsidence and filling ratio



under villages, there is a critical FR above which the buildings on the surface will be protected from the influence of mining. The influence of FR on surface subsidence varies with geology and mining conditions. In this study, the influence of FR can be summarized as follows.

Regardless of FR, the distribution pattern of the thickness of the injection body in the bed separation is determined when the grouting position is located in the region with the maximum subsidence. It is the S_{bmax} that changes with the variation of FR. According to Sect. 6.3, S_{bmax} comprises two parts: the reduction in surface subsidence and the compression to the caved rock. The ratio of surface subsidence reduction in the value of S_{bmax} is $1.102/1.88 = 0.586$, and therefore, final maximum surface subsidence after injection can be calculated as

$$S_{smax} = S_{sp} - 0.586S_{bmax} \tag{24}$$

Substituting Eq. (17) into Eq. (24), the surface subsidence changes into

$$S_{smax} = S_{sp} - \frac{0.586MW\alpha}{W - H/\tan\varphi} \tag{25}$$

Substituting $S_{sp} = 1.4$ m, $W = 145$ m, $H = 105$ m and $\varphi = 66.6^\circ$ into Eq. (25), then S_{smax} can be expressed as

$$S_{\text{max}} = 1.4 - 2.562\alpha. \quad (26)$$

Figure 17 depicts the relationship between final maximum surface subsidence and FR. Although Eq. (26) can be used to approximately predict final surface subsidence after injection, the actual relationship between S_{max} and α cannot be linear owing to the difference in the transfer of injection pressure upward and downward. Further study is needed regarding this issue, together with the distribution of the thickness of the injection body in the bed separation.

7 Conclusions

The improved GIBS technique was adopted for control of surface subsidence in actual mining under villages in the S104 mining section of the Liudian coal mine, China. Five boreholes were drilled from the surface to conduct the grout injection. During 3 years of operation, the total volume of compacted fly ash injected reached 169,651 m³ which accounts for 43.1 % of the gob volume.

Grout injection conducted in this manner has allowed the production of 850,000 t of coal at the study site, and yet, it has resulted in maximum surface subsidence of 0.298 m, which is only 10 % of the mining height and is 79 % less than predicted. Moreover, no damage has been found in the buildings of the overlying villages, either during or after extraction, and all the buildings currently remain stable. Finally, the unit cost of the injection is 30 RMB/t of coal, and up to 70 million RMB has been saved by conducting the grout injection project. Therefore, it can be concluded that the improved GIBS technique in this study is capable of bring significant economic and social benefits.

Acknowledgments The Graduate Education Innovation Projects of Jiangsu Province (CXLX11-0335) is greatly appreciated. The authors are grateful to the Huaibei Mining Group Co., Ltd. for their financial support for this research project at the China University of Mining and Technology. Particular thanks are due to Jianming Ni, Huaijun Yu and Kun Xu for their assistance with field tests. The thanks also go to anonymous reviewers for their constructive comments and suggestions.

References

- Abidin HZ, Djaja R, Darmawan D, Hadi S, Akbar A, Rajiyowiryono H, Sudibyo Y, Meilano I, Kasuma MA, Kahar J, Subarya C (2001) Land subsidence of Jakarta (Indonesia) and its geodetic monitoring system. *Nat Hazards* 23(2–3):365–387. doi:10.1023/A:1011144602064
- Bahuguna PP, Srivastava AMC, Saxena NC (1991) A critical review of mine subsidence prediction methods. *Min Sci Technol* 13(3):369–382. doi:10.1016/0167-9031(91)90716-P
- Bian Z, Miao X, Lei S, Chen S, Wang W, Struthers S (2012) The challenges of reusing mining and mineral-processing wastes. *Science* 337(6095):702–703. doi:10.1126/science.1224757
- Can E, Mekik Ç, Kuşçu Ş, Akçın H (2013) Monitoring deformations on engineering structures in Kozlu Hard Coal Basin. *Nat Hazards* 65(3):2311–2330. doi:10.1007/s11069-012-0477-x
- Chen SG, Guo H (2008) Numerical simulation of bed separation development and grout injecting into separations. *Geotech Geol Eng* 26(4):375–385. doi:10.1007/s10706-008-9174-7
- Chen SG, Hu W (2009) A comprehensive study on subsidence control using COSFLOW. *Geotech Geol Eng* 27(3):305–314. doi:10.1007/s10706-008-9230-3
- Deng K, Zhou M, Tan Z, Xu N (1998) Study on laws of rock mass breaking induced by mining. *J China Univ Min Technol* 27(3):261–264 (in Chinese)
- Guo H, Shen B, Chen S, Poole G (2005) Feasibility study of subsidence control using overburden grout injection technology. ACARP Project C12019, Australia
- Guo H, Shen B, Chen S (2007) Investigation of overburden movement and a grout injection trial for mine subsidence control. In: Proceedings and monographs in engineering, water and earth sciences, Vancouver, pp 1559–1566

- Harrison JP (2011) Mine Subsidence. In: Darling P (ed) SME mining engineering handbook, 3rd edn. Society for Mining, Metallurgy, and Exploration, Inc., Englewood
- Hsieh C, Shih T, Hu J, Tung H, Huang M, Angelier J (2011) Using differential SAR interferometry to map land subsidence: a case study in the Pingtung Plain of SW Taiwan. *Nat Hazards* 58(3):1311–1332. doi:[10.1007/s11069-011-9734-7](https://doi.org/10.1007/s11069-011-9734-7)
- Jia JY, Zhong YP, Wang SH, Zhang QS, Dong K (2008) Field measurements of bed separation in the overburden during longwall top coal caving under the railways. *Mine Surv* 04:59–62 (in Chinese)
- Jiřina T, Jan Š (2010) Reduction of surface subsidence risk by fly ash exploitation as filling material in deep mining areas. *Nat Hazards* 53(2):251–258. doi:[10.1007/s11069-009-9425-9](https://doi.org/10.1007/s11069-009-9425-9)
- Julio-Miranda P, Ortíz-Rodríguez AJ, Palacio-Aponte AG, López-Doncel R, Barboza-Gudiño R (2012) Damage assessment associated with land subsidence in the San Luis Potosi-Soledad de Graciano Sanchez metropolitan area, Mexico, elements for risk management. *Nat Hazards* 64(1):751–765. doi:[10.1007/s11069-012-0269-3](https://doi.org/10.1007/s11069-012-0269-3)
- Litwiniszyn J (1958) Statistical methods in the mechanics of granular bodies. *Rheol Acta* 1(2):146–150
- Liu BC, Liao GH (1965) Surface movements in coal mines. China Industry Publishing House, Beijing
- Luo Y, Peng SS, Zabrosky C, Cole J (2003) Mitigating subsidence influences on residential structures caused by longwall mining operations. In: Peng SS, Mark C, Khair AW (eds) Proceedings of the 22nd international conference on ground control, Morgantown, pp 352–359
- Luo Y, Ping SS, Mishra M (2004) Longwall mining under a mine refuse-disposal facility. *Min Eng* 56(9):89–93
- National Bureau of Statistics of China (2013) Statistical bulletin for national economic and social development 2012. http://www.stats.gov.cn/tjsj/tjgb/ndtjgb/qgndtjgb/201302/t20130221_30027.html. Accessed 8 Sept 2013
- Nie L, Zhang M, Jian H (2013) Analysis of surface subsidence mechanism and regularity under the influence of seism and fault. *Nat Hazards* 66(2):773–780. doi:[10.1007/s11069-012-0515-8](https://doi.org/10.1007/s11069-012-0515-8)
- Palarski J (1989) The experimental and practical results of applying backfill. In: Hassani FP, Scoble MJ, Yu TR (eds) Innovations in mining backfill technology. Balkema, Rotterdam, pp 33–37
- Palchik V (2003) Formation of fractured zones in overburden due to longwall mining. *Environ Geol* 44(1):28–38
- Palchik V (2005) Localization of mining-induced horizontal fractures along rock layer interfaces in overburden: field measurements and prediction. *Environ Geol* 48(1):68–80. doi:[10.1007/s00254-005-1261-y](https://doi.org/10.1007/s00254-005-1261-y)
- Palchik V (2010) Experimental investigation of apertures of mining-induced horizontal fractures. *Int J Rock Mech Min Sci* 47(3):502–508. doi:[10.1016/j.ijmms.2009.09.007](https://doi.org/10.1016/j.ijmms.2009.09.007)
- Peng SS, Chiang HS (1984) Longwall mining. Wiley, New York
- Siriwardane HJ, Kannan RS, Ziemkiewicz PF (2003) Use of waste materials for control of acid mine drainage and subsidence. *J Environ Eng* 129(10):910–915. doi:[10.1061/\(ASCE\)0733-9372\(2003\)129:10\(910\)](https://doi.org/10.1061/(ASCE)0733-9372(2003)129:10(910))
- State Bureau of Coal Industry (2000) Regulations of coal pillar design and extraction for buildings, water bodies, railways, main shafts and roadways. Coal Industry Press, Beijing
- Teng Y, Yan Z (1999) Study on law of overburden split developing in mining process. *J China Coal Soc* 24(01):27–30 (in Chinese)
- Xu J, Qian M, Yu H (2003) The characteristics of mining-induced fractures in overlying strata. In: Peng SS, Mark C, Khair Aw (eds) Proceedings of the 22nd international conference on ground control in mining, Morgantown, pp 44–47
- Xu Y, Shen S, Cai Z, Zhou G (2008) The state of land subsidence and prediction approaches due to groundwater withdrawal in China. *Nat Hazards* 45(1):123–135. doi:[10.1007/s11069-007-9168-4](https://doi.org/10.1007/s11069-007-9168-4)
- Xu H, Liu B, Fang Z (2014) New grey prediction model and its application in forecasting land subsidence in coal mine. *Nat Hazards* 71(2):1181–1194. doi:[10.1007/s11069-013-0656-4](https://doi.org/10.1007/s11069-013-0656-4)
- Yang L (2002) Re-understand the technology of reducing the subsidence due to mining by injecting grouts into separated beds in overlying disrupted strata by extraction. *J China Coal Soc* 27(4):352–356 (in Chinese)
- Zhao D, Fan X, Hong J, Qi D (1995) The application and effect of grout injection into the bed separation. *Coal Technol Northeast China* 05:9–12 (in Chinese)